Journal of Power Sources, 40 (1992) 291–298

Application of FeOCl derivatives as cathode materials for a secondary lithium battery
II. Comparison of the discharge and charge characteristics of γ-FeOOH prepared from the intercalation compound of FeOCl and 4-aminopyridine with those of FeOOH intercalated with aniline (a-FeOOH(AN))

Kiyoshi Kanamura, Hikari Sakaebe and Zen-ichiro Takehara

Department of Industrial Chemistry, Faculty of Engineering, Kyoto University, Yoshida-honmachi, Sakyo-ku, Kyoto 606-01 (Japan)

(Received January 13, 1992; in revised form June 30, 1992)

Abstract

The discharge and charge characteristics of γ-FeOOH products prepared from the intercalation compound of FeOCl and 4-aminopyridine were investigated in lithium cells and compared with those of FeOOH prepared from the intercalation compound of FeOCl and aniline (a-FeOOH(AN)). The polarization of γ-FeOOH cathode during the discharge and charge were larger than those of an a-FeOOH(AN) cathode. The electrochemical characteristics of the FeOOH products depend on the amorphous nature of the cathode material.

Introduction

Iron oxide compounds have been investigated as possible cathode and anode materials for the lithium batteries [1–3]. The discharge potentials of iron oxide cathodes are not high enough to provide the battery with a high-energy density. Although iron oxychloride (FeOCl) has been used as cathode material for lithium batteries [4, 5], the discharge product of FeOCl decomposes during discharge [6]. Therefore, FeOCl can not be utilized as cathode material for secondary lithium batteries. Recently, the modification of FeOCl was accomplished by ion exchange of Cl^- with OH^- in order to improve the rechargeability of the FeOCl cathode [7, 8]. The cyclability of this cathode was good enough for use in a practical cell. The final reaction product was assigned to amorphous FeOOH intercalated with aniline [8]. Similar modification to FeOCl may be carried out using other organic compounds as Lewis base [9].

In this study, the structure of FeOCl was modified using 4-aminopyridine to prepare the γ-FeOOH particles with a similar shape and size to FeOOH intercalated with aniline (a-FeOOH(AN)). The crystallinity of γ-FeOOH products and their discharge and charge characteristics in lithium cells were investigated and compared with those of the a-FeOOH(AN).

0378-7753/92/$5.00

Experimental

FeOCl was prepared according to ref. 6. The preparation of γ-FeOOH was conducted by ion exchange of Cl^- of FeOCl with OH^-. FeOCl, however, does not uniformly exchange Cl^- for OH^- in alkaline aqueous solutions. Therefore, the intercalation compound of FeOCl and 4-aminopyridine was prepared as an intermediate, which has high reactivity with OH^-. FeOCl and 4-aminopyridine were put into a pyrex tube with the molar ratio of 4:1. Acetone was used as the solvent. The pyrex tube was evacuated and sealed. The bottom of a pyrex tube was immersed in an oil bath at 373 K for 7 days. The reaction product was washed with acetone and dried under vacuum at 353 K. The product (5 g) was immersed into 0.1 M LiOH solution (250 cm^3) at 313 K for 1 day. The product was washed with water and then dried under vacuum at 353 K for more than 2 days. On the other hand, a-FeOOH(AN) was prepared from the intercalation compound of FeOCl and aniline. FeOCl and aniline in a mole ratio of 4:1 were immersed in water for 3 days at 303 K with stirring of the solution under argon atmosphere. The reaction product was washed with water and acetone and dried under vacuum at 373 K for more than 2 days. The products were analyzed by X-ray diffraction and infrared spectroscopy.

The discharge and charge characteristics of the two FeOOH types cathodes were evaluated in lithium cells. The FeOOH product, acetylene black, and polytetrafluoroethylene (PTFE) were mixed in a weight ratio of 50:45:5 and then pressed at 2.98×10^8 Pa to make the cathode pellet. Lithium metal was used as counter and reference electrodes. Propylene carbonate with 1.0 M $LiBF_4$ was used as the electrolyte. The electrochemical measurements were conducted in an argon dry box at 300 K.

Results and discussion

Figure 1(a) shows the X-ray diffraction pattern of FeOCl intercalated with 4-aminopyridine. The main peak was observed at $2\theta = 6.545°$, which corresponds to an interlayer distance of 1.3492 nm. The interlayer distance of FeOCl used as the starting material was about 0.8 nm. The expanded interlayer distance indicates that 4-aminopyridine has intercalated into FeOCl to form the intercalation compound. Figure 1(b) shows the X-ray diffraction pattern of the final product which is very different from the pattern (a). All peaks in pattern (b) were assigned to those of γ-FeOOH [8]. The change of the X-ray diffraction pattern from Fig. 1(a) to (b) corresponds to the ion exchange reaction of Cl^- with OH^- and removal of 4-aminopyridine from the structure. The contents of Fe and Cl^- in the product were determined to be 0.92% in weight (molar ratio between Fe and Cl is estimated to be 1:0.02) by chemical analysis and atomic absorption. The intensity of the main peaks at $2\theta = 14.04°$ in two types FeOOH were much weaker than that of FeOCl [7, 8]. This means that the γ-FeOOH (Fig. 1(b)) and a-FeOOH(AN) (Fig. 1(c)) prepared in this study are less crystalline than that FeOCl.

When Cl^- was exchanged with OH^- in the intercalation compound of FeOCl and aniline, the aniline remained in the product [7, 8]. In the case of the intercalated product of γ-FeOOH and 4-aminopyridine, the latter can dissolve in an aqueous solution and therefore be extracted from the product. Figure 2 shows the infrared spectra (a–d) of the intercalation compounds of FeOCl and 4-aminopyridine or aniline and the final products, respectively. In the spectra (a) and (b), the absorption peak near 500 cm^{-1} corresponds to the Fe–O bond in FeOCl. The peaks from 700 cm^{-1}

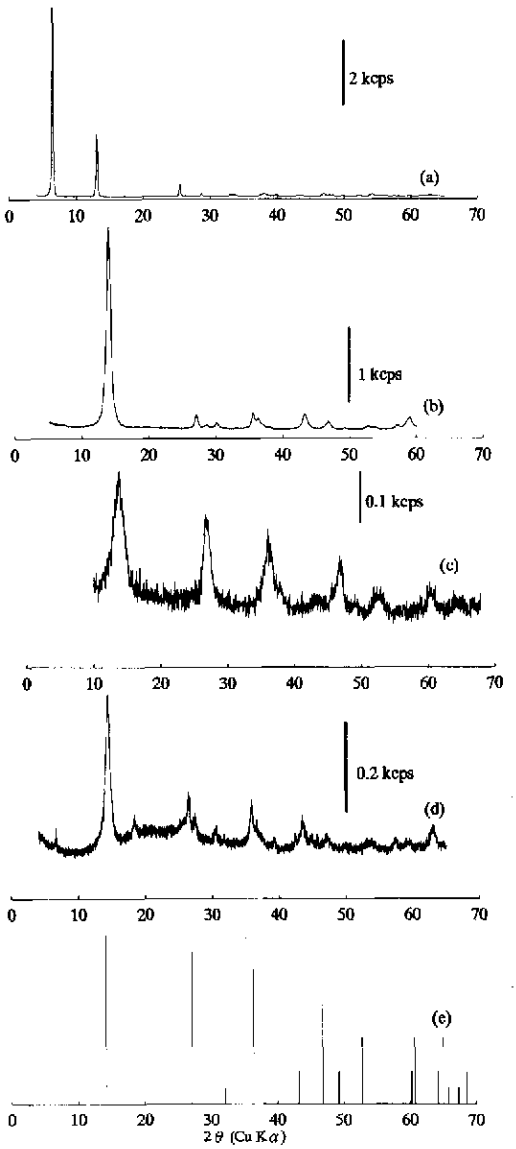

Fig. 1. X-ray diffraction patterns of (a) the intercalation compound of FeOCl and 4-aminopyridine, (b) γ-FeOOH prepared by the ion exchange of Cl^- of FeOCl with OH^-, (c) a-FeOOH(AN) prepared by the ion exchange of Cl^- with OH^-, (d) γ-FeOOH after the second discharge and charge cycle, and (e) γ-FeOOH reported in JCPDS 8-98.

to 1600 cm^{-1} correspond to 4-aminopyridine or aniline. Therefore, the spectra (a) and (b) indicate that the product consists of FeOCl and 4-aminopyridine and aniline, respectively. In the spectra (c), the two peaks near 500 cm^{-1} correspond to the bonds of Fe–O and Fe–OH. The peaks at 700 cm^{-1}, 1000 cm^{-1}, and 3000 cm^{-1} are assigned to an O–H bond. The peaks from 700 cm^{-1} to 1600 cm^{-1} observed in the

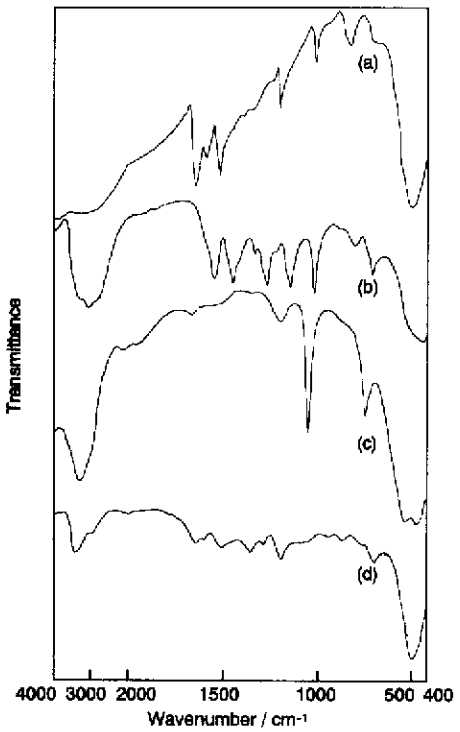

Fig. 2. Infrared spectra of (a) the intercalation compound of FeOCl and 4-aminopyridine, (b) the intercalation compound of FeOCl and aniline, (c) γ-FeOOH prepared by the ion exchange of Cl^- of FeOCl with OH^-, and (d) a-FeOOH(AN) prepared by the ion exchange of Cl^- of FeOCl with OH^-.

spectrum (a) are not present in the spectrum (c). It is therefore concluded that the intercalated 4-aminopyridine is extracted from FeOCl during the ion exchange process. Spectrum (d) is that of a-FeOOH(AN). Several absorption peaks were observed in the region from 800 to 1600 cm^{-1} and correspond to aniline that remains in the host matrix. The peak at 500 cm^{-1} corresponds to the Fe–O bond and Fe–OH bond. However, only one broad peak was observed in spectrum (d). This is clearly different from the spectra of γ-FeOOH and indicates that the bond strength between Fe and O is similar to that between Fe and OH. Therefore it can be concluded that the crystal structure around the Fe atom in a-FeOOH(AN) is different from that of γ-FeOOH. Such a fine structural difference may influence the discharge and charge characteristics of the FeOOH cathode.

The crystal shape and size influence the discharge and charge characteristics of the cathode. In order to compare the discharge and charge characteristics of the a-FeOOH(AN) cathode with a γ-FeOOH cathode, both FeOOH compounds were prepared from the same FeOCl precursor. Scanning electron micrographs of a-FeOOH(AN) and γ-FeOOH show that the particles in both products are similar and have a planar morphology (Fig. 3).

Figure 4 shows the discharge and charge curves of cell containing γ-FeOOH at various current rates. The discharge capacity obtained at 0.13 mA cm^{-2} (curve d)

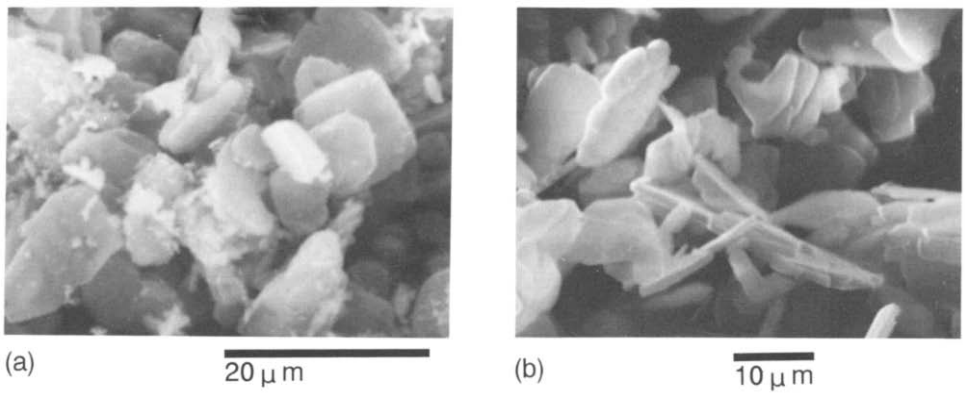

Fig. 3. Scanning electron micrographs of (a) γ-FeOOH prepared by the ion exchange of Cl^- of FeOCl with OH^- and (b) a-FeOOH(AN) prepared by ion exchange of Cl^- of FeOCl with OH^-.

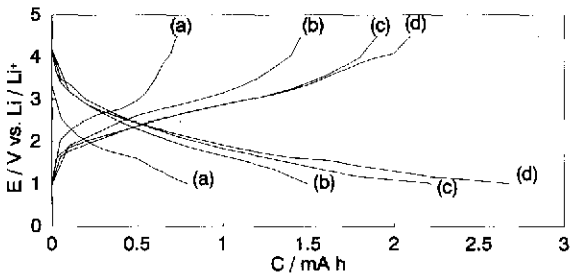

Fig. 4. Discharge and charge curves of γ-FeOOH in propylene carbonate containing 1.0 M $LiBF_4$ at various current densities, (a) 1.27 mA cm^{-2}, (b) 0.64 mA cm^{-2}, (c) 0.25 mA cm^{-2}, and (d) 0.13 mA cm^{-2}; discharge cutoff voltage: 1.5 V vs. Li/Li^+ and charge cutoff voltage: 4.5 V vs. Li/Li^+.

was approximately three times as large as that at 1.27 mA cm^{-2} (curve a). From the strong dependence of the discharge capacity on current density, it can be seen that the discharge capacity is effected by the electrochemical kinetics of the cathode, which may be related to the diffusion of lithium in the γ-FeOOH structure.

Figure 5 shows the discharge and charge capacities of the γ-FeOOH product during the discharge and charge cycles at various current densities. The discharge capacity decreased with an increasing in the discharge current. The discharge capacity increased with the cycle during the initial 6 cycles (region I), which was attributed to a decrease in a polarization of the cathode. This behavior is due to the structural change of the γ-FeOOH caused by successive lithium insertion and extraction reactions. Figure 1(d) shows the X-ray diffraction pattern of the γ-FeOOH after the second discharge and charge cycle. The intensities of all peaks decreased after the discharge and charge cycle. From this results, it can be seen that the γ-FeOOH structure becomes less crystalline. In the region IV, the amount of electricity in the charge process (Q_c) was the same as that in the discharge (Q_d). In regions II and III, Q_c was smaller than Q_d, indicating that part of the lithium inserted into γ-FeOOH during discharge could not be extracted from the structure during the charge. In region V, Q_c was

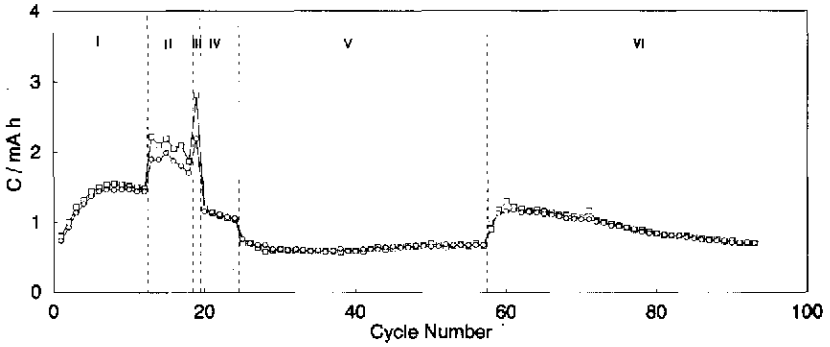

Fig. 5. (○) Discharge and (□) charge capacities of γ-FeOOH at various current densities: region I 0.64 mA cm^{-2}, region II 0.25 mA cm^{-2}, region III 0.13 mA, region IV 0.64 mA cm^{-2}, region V 1.27 mA cm^{-2}, and region VI 0.64 mA cm^{-2}.

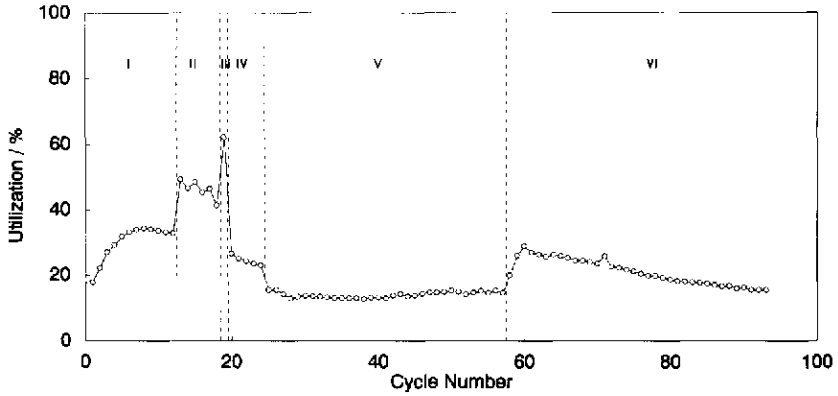

Fig. 6. Utilization of γ-FeOOH at various current densities: region I 0.64 mA cm^{-2}, region II 0.25 mA cm^{-2}, region III 0.13 mA cm^{-2}, region IV 0.64 mA cm^{-2}, region V 1.27 mA cm^{-2}, and region VI 0.64 mA cm^{-2}.

nearly equal to Q_d. The discharge capacity in region IV gradually decreased with increasing cycle number. From the ratio of Q_c/Q_d which decreases with decreasing discharge and charge current densities, it was concluded that the rechargeability of the γ-FeOOH cathode was related to the depth-of-discharge. The maximum amount of lithium that is inserted into, and extracted from the γ-FeOOH reversibly is less than 0.2. Figure 6 shows the cathode utilization as a function of cycle number, as determined from Fig. 5. The utilization in the regions I, IV, and VI (the discharge current density = 0.64 mA cm^{-2}) ranged from 20 to 35%. By contrast, the utilization in region II was 62%. The utilization in the region V (discharge current density = 1.27 mA cm^{-2}) was 15%. The rechargeability of the cathode in this region was very stable. The lower utilization of the cathode at the high-current discharge was attributed to the slow diffusion of lithium in the cathode.

Figure 7 shows the discharge and charge curves of Li/a-FeOOH(AN) cells obtained at various current rates. The discharge potentials and cell capacities are significantly higher than those of Li/γ-FeOOH cells. Furthermore, a-FeOOH(AN) cathodes perform better at higher current density than the γ-FeOOH cathodes. These results indicate

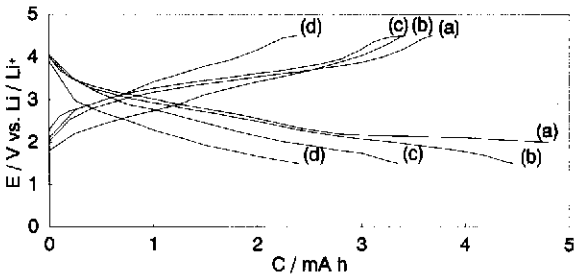

Fig. 7. Discharge and charge curves of a-FeOOH(AN) in propylene carbonate containing 1.0 M $LiBF_4$ at various current densities: (a) 0.64 mA cm^{-2}, (b) 1.27 mA cm^{-2}, (c) 2.55 mA cm^{-2}, and (d) 5.1 mA cm^{-2}.

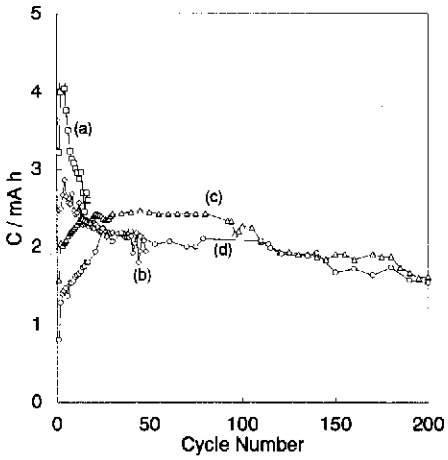

Fig. 8. Discharge capacities of a-FeOOH(AN) in propylene carbonate containing 1.0 M $LiBF_4$: (a) 0.64 mA cm^{-2}, (b) 1.27 mA cm^{-2}, (c) 2.55 mA cm^{-2}, and (d) 5.1 mA cm^{-2}.

that the diffusion of lithium is significant faster in a-FeOOH(AN) than that in γ-FeOOH.

Figure 8 shows the discharge capacities of a-FeOOH(AN) at various discharge current densities. The variation of the discharge capacity, as a function of cycle number that shows an increase in the initial cycles and then a gradual decrease, was similar to that in the γ-FeOOH. The discharge capacity of a-FeOOH(AN) at 5.1 mA cm^{-2} was 2 mA h at the 200th cycle which corresponds to a capacity utilization between 60 and 70%. This value is much larger than that obtained from γ-FeOOH cathodes.

Conclusion

Although both a-FeOOH(AN) and the γ-FeOOH have the γ-FeOOH network structure, it appears that the resident intercalated organic compound and the degree of crystallinity of the cathodes are factors that are responsible for the difference in performance of a-FeOOH(AN) and γ-FeOOH electrodes. In addition, it is believed that differences in the Fe–O and Fe–OH chemical bond structure may influence the

discharge and charge characteristics of the FeOOH cathode. It is therefore concluded that a-FeOOH(AN) is a superior cathode to γ-FeOOH and that an a-FeOOH(AN) electrode with the best performance and highest energy density will be obtained by optimizing the amount of aniline in the structure and the degree of crystallinity of the cathode material.

References

1 M. M. Thackeray and J. Coetzer, *Mater. Res. Bull., 16* (1981) 591.
2 L. A. de Picciotto and M. M. Thackeray, *Mater. Res. Bull., 21* (1986) 583.
3 M. M. Thackeray, W. I. F. David and J. B. Goodenough, *Mater. Res. Bull., 17* (1981) 785.
4 S. Kikkawa, T. Yamamoto and M. Loizumi, *Yogyo Kyokaishi, 93* (1985) 311.
5 H. Meyer, A. Weiss and J. O. Besenhard, *Mater. Res. Bull., 13* (1982) 913.
6 Z. Takehara, K. Kanamura, N. Imanishi and C. Zhen, *Bull. Chem. Soc. Jpn., 62* (1989) 3609.
7 K. Kanamura, C. Zhen, H. Sakaebe and Z. Takehara, *J. Electrochem. Soc., 138* (1991) 331.
8 K. Kanamura, C. Zhen, H. Sakaebe and Z. Takehara, *J. Electrochem. Soc.,* to be submitted.
9 K. Kanamura, N. Imanishi, M. Fujiwara and Z. Takehara, *J. Power Sources, 26* (1989) 467.